Composite Structures 105 (2013) 75–81

Contents lists available at SciVerse ScienceDirect

Composite Structures

journal homepage: www.elsevier.com/locate/compstruct

Analysis of composite plates by a unified formulation-cell based smoothed finite element method and field consistent elements

S. Natarajan [a,*], A.J.M. Ferreira [b,c], S.P.A. Bordas [d], E. Carrera [e], M. Cinefra [e]

[a] School of Civil and Environmental Engineering, University of New South Wales, Australia
[b] Universidade do Porto, Faculdade de Engenharia, Porto, Portugal
[c] Department of Mathematics, Faculty of Science, King Abdulaziz University, Jeddah, Saudi Arabia
[d] Institute of Mechanics and Advanced Materials, Cardiff University, Wales, UK
[e] Department of Aeronautics and Aerospace Engineering, Politecnico di Torino, Italy

ARTICLE INFO

Article history:
Available online 14 May 2013

Keywords:
Carrera's unified formulation
Cell-based smoothed finite element method
Field consistency
Shear locking
Laminated composites
Sinusoidal theory

ABSTRACT

In this article, we combine Carrera's Unified Formulation (CUF) [13,7] and cell based smoothed finite element method [28] for studying the static bending and the free vibration of thin and thick laminated plates. A 4-noded quadrilateral element based on the field consistency requirement is used for this study to suppress the shear locking phenomenon. The combination of cell based smoothed finite element method and field consistent approach with CUF allows a very accurate prediction of field variables. The accuracy and efficiency of the proposed approach are demonstrated through numerical experiments.
© 2013 Elsevier Ltd. All rights reserved.

1. Introduction

With the rapid development of engineering, there is an increasing demand for new materials suited for harsh working environments. Engineered materials such as composite materials are used in the construction of aeronautical and aerospace vehicles, as well as civil and mechanical structures. This is because of their excellent strength-to and stiffness-to-weight ratios and the possibility of tailoring their properties to optimize the structural response. However, the analysis of such structures is a complex task, compared with conventional single layer metallic structures. This is because of coupling between membrane, torsion and bending strains; weak transverse shear rigidities; and discontinuity of the mechanical characteristics through the thickness of the laminates. For these reasons, accurate modeling and simulating the characteristics of composite structures through different higher-order displacement functions for two-dimensional theories is taking an important part of mechanics and materials research. Indeed two dimensional theories lead to much less expensive models compared to three-dimensional theories. In this context, analytical/numerical methods based on various 2D higher-order theories for static and dynamic analyses of rectangular laminates have been the subject of increasing attention in the research community.

Various structural theories proposed for evaluating the characteristics of composite laminates under different loading situations were reviewed by [38,29,19] and recently by Khanda et al. [21]. In general, three different approaches have been used to study laminated composite structures: single layer theories, discrete layer theories and mixed plate theory. In the single layer theory approach, layers in laminated composites are assumed to be one equivalent single layer (ESL), whereas in the discrete layer theory approach, each layer is considered in the analysis. Although the discrete layer theories provide very accurate prediction of the displacements and the stresses, increasing the number of layers increases the number of unknowns. This can be prohibitively costly and significantly increase the computational time [48]. To overcome the above limitation, zig–zag models developed by Murukami [30] can satisfy the transverse shear stresses continuity conditions at the interfaces. Moreover, the number of unknowns are independent of the number of layers. Reddy and Robbins [42] presented a review of various equivalent-single-layer and layer-wise laminated plate theories and their finite element models.

Recently, some researchers have attempted to combine single layer theories and discrete layer theories to overcome the limitations of each one. Carrera [13,31,7] derived a series of axiomatic approaches, coined as 'Carrera Unified Formulation' (CUF) for the general description of two-dimensional formulations for multilayered plates and shells. With this unified formulation it is possible to implement in a single software a series of hierarchical formulations, thus affording a systematic assessment of different theories,

* Corresponding author. Tel.: +61 293855656.
E-mail address: sundararajan.natarajan@gmail.com (S. Natarajan).

0263-8223/$ - see front matter © 2013 Elsevier Ltd. All rights reserved.
http://dx.doi.org/10.1016/j.compstruct.2013.04.040

ranging from simple ESL models up to higher order layerwise descriptions. This formulation is a valuable tool for gaining a deep insight into the complex mechanics of laminated structures.

The CUF has been used to develop discrete models such as the finite element method (FEM) [13,31], and more recently, meshless methods based upon collocation with radial basis functions [16]. Although the FEM provides a general and systematic technique for constructing basis functions, difficulties still exist in the development of plate elements based on shear deformation theories, one of which is the shear locking phenomenon. Different techniques by which the locking phenomena can be suppressed include: (a) retain the original interpolations and use an optimal integration rule [18]; (b) assumed natural strain method [1,45] and (c) enhanced assumed strain method [44]. Recently, Cinefra et al. employed mixed interpolation of tensorial components (MITC) technique for 4-noded [8] and 9-noded [10–12] multilayered shell/plate elements formulated on the basis of CUF.

Another set of methods have emerged to address the shear locking in the FEM. By incorporating the strain smoothing technique into the finite element method (FEM), Liu et al. [28] have formulated a series of smoothed finite element methods (SFEMs), named as cell-based SFEM (CS-FEM) [34,4], node-based SFEM [26], edge-based SFEM [25], face-based SFEM [33] and α-FEM [24]. And recently, edge based imbricate finite element method (EI-FEM) was proposed in [9] that shares common features with the ES-FEM. As the SFEM can be recast within a Hellinger–Reissner variational principle, suitable choices of the assumed strain/gradient space provides stable solutions. Depending on the number and geometry of the subcells used, a spectrum of methods exhibiting a spectrum of properties is obtained. Interested are referred to the literature [27,34] and references therein. Nguyen-Xuan et al. [37] employed CS-FEM for Mindlin–Reissner plates. The curvature at each point is obtained by a non-local approximation via a smoothing function. From the numerical studies presented, it was concluded that the CS-FEM technique is robust, computationally inexpensive, free of locking and importantly insensitive to mesh distortions. The SFEM was extended to various problems such as shells [35], heat transfer [49], fracture mechanics [36] and structural acoustics [17] among others. In [3], CS-FEM has been combined with the extended FEM to address problems involving discontinuities.

In this study, a $\mathcal{C}^0$ 4-noded quadrilateral element is employed to study the static bending and free vibration of laminated composites. The plate kinematics is based on Carrera Unified Formulation (CUF) and a sinusoidal shear deformation theory is used to approximate the displacements. A CS-FEM with field consistency approach is employed to study the response of laminated composites. The influence of various parameters, viz., the thickness of the plate, the fiber orientation, the ply lay up and the material properties on the response of the laminated composite plates is studied numerically.

The paper is organized as follows. Section 2 presents an overview of the Unified Formulation, the finite element discretization and the cell-based smoothing technique for implementation of the CUF. A discussion on computing the fundamental nuclei is also given. The results of the present formulation are compared with those available in the literature in Section 3, bringing out the influence of various parameters on the static bending and the natural frequencies, followed by concluding remarks in the last section.

2. Carrera unified formulation

2.1. Basis of CUF

Let us consider a laminated plate composed of perfectly bonded layers with coordinates x, y along the in-plane directions and z along the thickness direction of the whole plate, while z_k is the thickness of the kth layer. The CUF is a useful tool to implement a large number of two-dimensional models with the description at the layer level as the starting point. By following the axiomatic modeling approach, the displacements $\mathbf{u}(x,y,z) = (u(x,y,z),\ v(x,y,z),\ w(x,y,z))$ are written according to the general expansion as:

$$\mathbf{u}(x,y,z) = \sum_{\tau=0}^{N} F_\tau(z)\mathbf{u}_\tau(x,y) \tag{1}$$

where $F(z)$ are known functions to model the thickness distribution of the unknowns, N is the order of the expansion assumed for the through-thickness behavior. By varying the free parameter N, a *hierarchical* series of two-dimensional models can be obtained. The strains are related to the displacement field via the geometrical relations:

$$\begin{aligned}\boldsymbol{\varepsilon}_{pG} &= \begin{bmatrix}\varepsilon_{xx} & \varepsilon_{yy} & \gamma_{xy}\end{bmatrix}^{\mathrm{T}} = \mathbf{D}_p\mathbf{u}\\ \boldsymbol{\varepsilon}_{nG} &= \begin{bmatrix}\gamma_{xz} & \gamma_{yz} & \varepsilon_{zz}\end{bmatrix}^{\mathrm{T}} = (\mathbf{D}_{np}+\mathbf{D}_{nz})\mathbf{u}\end{aligned} \tag{2}$$

where the subscript G indicate the geometrical equations, $\mathbf{D}_p$, $\mathbf{D}_{np}$ and $\mathbf{D}_{nz}$ are differential operators given by:

$$\mathbf{D}_p = \begin{bmatrix}\partial_x & 0 & 0\\ 0 & \partial_y & 0\\ \partial_y & \partial_x & 0\end{bmatrix},\quad \mathbf{D}_{np} = \begin{bmatrix}0 & 0 & \partial_x\\ 0 & 0 & \partial_y\\ 0 & 0 & 0\end{bmatrix},\quad \mathbf{D}_{nz} = \begin{bmatrix}\partial_z & 0 & 0\\ 0 & \partial_z & 0\\ 0 & 0 & \partial_z\end{bmatrix}. \tag{3}$$

The 3D constitutive equations are given as:

$$\begin{aligned}\boldsymbol{\sigma}_{pC} &= \mathbf{C}_{pp}\boldsymbol{\varepsilon}_{pG} + \mathbf{C}_{pn}\boldsymbol{\varepsilon}_{nG}\\ \boldsymbol{\sigma}_{nC} &= \mathbf{C}_{np}\boldsymbol{\varepsilon}_{pG} + \mathbf{C}_{nn}\boldsymbol{\varepsilon}_{nG}\end{aligned} \tag{4}$$

with

$$\begin{aligned}\mathbf{C}_{pp} &= \begin{bmatrix}C_{11} & C_{12} & C_{16}\\ C_{12} & C_{22} & C_{26}\\ C_{16} & C_{26} & C_{66}\end{bmatrix}\mathbf{C}_{pn} = \begin{bmatrix}0 & 0 & C_{13}\\ 0 & 0 & C_{23}\\ 0 & 0 & C_{36}\end{bmatrix}\\ \mathbf{C}_{np} &= \begin{bmatrix}0 & 0 & 0\\ 0 & 0 & 0\\ C_{13} & C_{23} & C_{36}\end{bmatrix}\mathbf{C}_{nn} = \begin{bmatrix}C_{55} & C_{45} & 0\\ C_{45} & C_{44} & 0\\ 0 & 0 & C_{33}\end{bmatrix}\end{aligned} \tag{5}$$

where the subscript C indicate the constitutive equations. The *Principle of Virtual Displacements* (PVDs) in case of multilayered plate subjected to mechanical loads is written as:

$$\begin{aligned}&\sum_{k=1}^{N_k}\int_{\Omega_k}\int_{A_k}\left\{\left(\delta\boldsymbol{\varepsilon}_{pG}^k\right)^{\mathrm{T}}\boldsymbol{\sigma}_{pC}^k + \left(\delta\boldsymbol{\varepsilon}_{nG}^k\right)^{\mathrm{T}}\boldsymbol{\sigma}_{nC}^k\right\}\mathrm{d}\Omega_k\mathrm{d}z\\ &\quad= \sum_{k=1}^{N_k}\int_{\Omega_k}\int_{A_k}\rho^k\delta\mathbf{u}_s^{k^{\mathrm{T}}}\ddot{\mathbf{u}}^k\mathrm{d}\Omega_k\ \mathrm{d}z + \sum_{k=1}^{N_k}\delta\mathbf{L}_e^k\end{aligned} \tag{6}$$

where ρ^k is the mass density of the kth layer, Ω_k, A_k are the integration domain in the (x,y) and the z direction, respectively. Upon substituting the geometric relations (Eq. (2)), the constitutive relations (Eq. (4)) and the unified formulation into the PVD statement, we have:

$$\begin{aligned}&\int_{\Omega_k}\int_{A_k}\left\{\left(\mathbf{D}_p^k F_s\delta\mathbf{u}_s^k\right)^{\mathrm{T}}\left\{\mathbf{C}_{pp}^k\mathbf{D}_p^k F_\tau\mathbf{u}_\tau^k + \mathbf{C}_{pn}^k\left(\mathbf{D}_{n\Omega}^k + \mathbf{D}_{nz}^k\right)F_\tau\mathbf{u}_\tau^k\right\}\right.\\ &\left.+\left[\left(\mathbf{D}_{n\Omega}^k + \mathbf{D}_{nz}^k\right)f_x\delta\mathbf{u}_s^k\right)^{\mathrm{T}}\left(\mathbf{C}_{np}^k\mathbf{D}_p^k F_\tau\mathbf{u}_\tau^k + \mathbf{C}_{nn}^k\left(\mathbf{D}_{n\Omega}^k + \mathbf{D}_{nz}^k\right)F_\tau\mathbf{u}_\tau^k\right)\right]\right\}\mathrm{d}\Omega_k\mathrm{d}z\\ &= \sum_{k=1}^{N_k}\int_{\Omega_k}\int_{A_k}\rho^k\delta\mathbf{u}_s^{k^{\mathrm{T}}}\ddot{\mathbf{u}}^k\mathrm{d}\Omega_k\mathrm{d}z + \sum_{k=1}^{N_k}\delta\mathbf{L}_e^k\end{aligned} \tag{7}$$

After integration by parts, the governing equations for the plate are obtained:

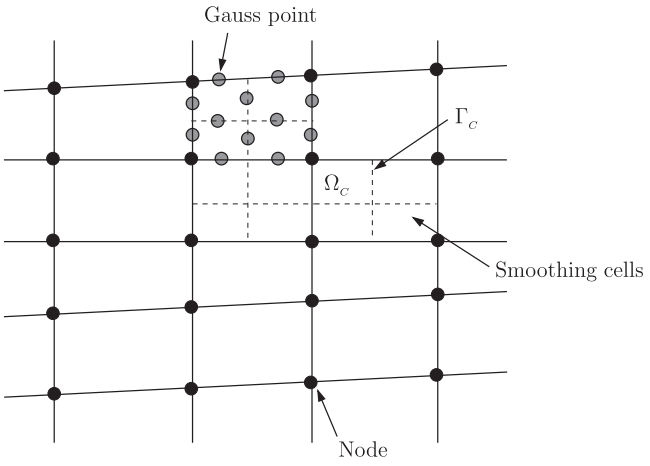

Fig. 1. Example of finite element meshes and smoothing cells. The integration is performed along the boundary of each subcell. The smoothing cells, Ω_C and Γ_C is the boundary of the subcell.

$$\mathbf{K}_{uu}^{k\tau s}\mathbf{u}_{\tau}^{k} = \mathbf{P}_{u\tau}^{k} \tag{8}$$

and in the case of free vibrations, we have:

$$\mathbf{K}_{uu}^{k\tau s}\mathbf{u}_{\tau}^{k} = \mathbf{M}^{k\tau s}\ddot{\mathbf{u}}_{\tau}^{k} \tag{9}$$

where the fundamental nucleus $\mathbf{K}_{uu}^{k\tau s}$ is:

$$\mathbf{K}_{uu}^{k\tau s} = \left[\left(-\mathbf{D}_{p}^{k}\right)^{\mathrm{T}}\left(\mathbf{C}_{pp}^{k}\mathbf{D}_{p}^{k} + \mathbf{C}_{pn}^{k}\left(\mathbf{D}_{n\Omega}^{k} + \mathbf{D}_{nz}\right)\right) + \left(-\mathbf{D}_{n\Omega}^{k} + \mathbf{D}_{nz}^{k}\right)^{\mathrm{T}}\left(\mathbf{C}_{np}^{k}\mathbf{D}_{p}^{k} + \mathbf{C}_{nn}^{k}\left(\mathbf{D}_{n\Omega}^{k} + \mathbf{D}_{nz}^{k}\right)\right)\right]F_{\tau}F_{s} \tag{10}$$

and $\mathbf{M}^{k\tau s}$ is the fundamental nucleus for the inertial term given by:

$$M_{ij}^{k\tau s} = \begin{cases} \rho^{k}F_{\tau}F_{s} & \text{if } i = j \\ 0 & \text{if } i \neq j \end{cases} \tag{11}$$

where $\mathbf{P}_{u\tau}^{k}$ are variationally consistent loads with applied pressure. For more detailed derivation and for the explicit form of the fundamental nuclei, interested readers are referred to [13,31].

2.2. Element description

The plate element employed in this study is a C^0 continuous element and according to the isoparametric description, the components of each displacement unknown $\mathbf{u}_{\tau}$ are expressed as:

$$\mathbf{u}_{\tau} = N_I\mathbf{q}_{\tau I}, \quad I = 1, 2, \ldots, N_n \tag{12}$$

where N_I are the standard finite element shape functions. By introducing the unified formulation for the displacements, given by Eq. (12) into the strain–displacement relations (see Eq. (2)), we have:

$$\begin{aligned} \boldsymbol{\varepsilon}_{pG}^{k} &= \mathbf{D}_{p}^{k}\left(F_{\tau}\mathbf{u}_{\tau}^{k}\right) = \mathbf{D}_{p}^{k}(F_{\tau}N_I)\mathbf{q}_{\tau I}^{k} \\ \boldsymbol{\varepsilon}_{nG}^{k} &= \left(\mathbf{D}_{n\Omega}^{k} + \mathbf{D}_{nz}^{k}\right)\left(F_{\tau}\mathbf{u}_{\tau}^{k}\right) = \mathbf{D}_{n\Omega}^{k}(F_{\tau}N_I)\mathbf{q}_{\tau I}^{k} + F_{\tau,z}N_I\mathbf{q}_{\tau I}^{k} \end{aligned} \tag{13}$$

Upon substituting Eqs. (12) and (13) into Eqs. (10) and (11), we can compute the stiffness and the mass matrix of the system. The formulation is implemented in MATLAB and the solution to the static bending is computed by Gauss-elimination algorithm and the solution to free vibration problem is computed from a standard eigenvalue algorithm.

2.3. Overview of the gradient smoothing method in finite elements

In the following, the gradient smoothing method is briefly reviewed. For more detailed discussion, readers are referred to the literature and the references therein [34,4]. The stabilized conforming nodal integration was proposed in [14], where the strain is written as the divergence of a spatial average of the standard (compatible) strain field – i.e., symmetric gradient of the displacement field. In the FE version of the gradient smoothing method, the domain is partitioned/decomposed into subcells (see Fig. 1). One way to create subcell geometries is to decompose directly the elements of an existing mesh, the simplest decomposition being realized where each subcell coincides with an element. Other node, edge and face-based decomposition techniques were proposed in a number of papers [24,26,25,33]. The strain field, $\tilde{\varepsilon}_{ij}^{h}$ used to compute the stiffness matrix is computed by a weighted average of the standard strain field ε_{ij}^{h}. At a point $\mathbf{x}_C$ in an element Ω^h, the smoothed strain field is given by:

$$\tilde{\varepsilon}_{ij}^{h} = \int_{\Omega^h} \varepsilon_{ij}^{h}(\mathbf{x})\Phi(\mathbf{x} - \mathbf{x}_C)\mathrm{d}\mathbf{x} \tag{14}$$

where Φ is a smoothing function that generally satisfies the following properties:

$$\Phi \geqslant 0 \text{ and } \int_{\Omega^h} \Phi(\mathbf{x})\mathrm{d}\mathbf{x} = 1 \tag{15}$$

One possible choice of Φ is given by

$$\Phi = \begin{cases} \frac{1}{A_C} & \mathbf{x}_C \in \Omega_C \\ 0 & \mathbf{x}_C \notin \Omega_C \end{cases}$$

where A_C is the area of the subcell. This process of smoothing the gradient field is called as *'cell-based smoothed finite element method'* (CS-FEM) in the literature [34,4]. The SFEM can be recast within a Hellinger–Reissner variational principle, where the assumed strain is the (constant) smoothed strain over each subcell. For stability, the approximation of the smoothed strain and of the displacement field must satisfy the LBB condition [2].

2.4. In-plane strain

In this article, we apply the smoothing technique to the in-plane strains by a divergence estimation via a spatial averaging of the strain fields as explained earlier. In other words, the domain integrals are transformed into boundary integrals. This smoothing technique avoids the evaluation of the derivatives of the shape functions and thus avoiding the iso-parametric mapping. The smoothing is performed over arbitrary smoothing cell, Ω_C, illustrated in Fig. 1 with boundary $\Gamma_C = \bigcup_{b=1}^{nb}\Gamma_C^b$, where Γ_C^b is the boundary segment of Ω_C and nb is the total number of edges of each smoothing cell. The relation between the smoothed in-plane strain and the nodal displacements is given by:

$$\tilde{\boldsymbol{\varepsilon}}_{pG}^{k} = \tilde{\mathbf{D}}_{pC}^{k}\mathbf{q}_{\tau I}^{k} \tag{16}$$

where $\tilde{\mathbf{D}}_{pC}^{k}$ is the smoothed strain–displacement matrix, given by:

$$\tilde{\mathbf{D}}_{pC}^{k} = \frac{1}{A_C}\int_{\Gamma_C} F_{\tau}N_I\begin{bmatrix} n_x & 0 & 0 \\ 0 & n_y & 0 \\ n_y & n_x & 0 \end{bmatrix}\mathrm{d}\Gamma \tag{17}$$

Table 1
Convergence of the central deflection $\bar{w} = w(a/2, a/2, 0)\frac{100E_2h^3}{Pa^4}$ of a simply supported cross-ply laminated square plate [0°/90°/90°/0°] with $E_1 = 25E_2$, $G_{12} = G_{13} = 0.5E_2$, $G_{23} = 0.2E_2$, $\nu_{12} = 0.25$.

Mesh	FEM-Q4	CSFEM-Q4		
		1 Subcell	2 Subcells	4 Subcells
8×8	0.4351	0.4405	0.4398	0.4365
10×10	0.4330	0.4364	0.4360	0.4339
14×14	0.4312	0.4329	0.4327	0.4316
20×20	0.4302	0.4310	0.4309	0.4304
30×30	0.4297	0.4301	0.4300	0.4298

Table 2
The normalized central deflection $\bar{w} = w(a/2, a/2, 0)\frac{100E_2h^3}{Pa^4}$, stresses, $\bar{\sigma}_{xx} = \sigma_{xx}(a/2, a/2, h/2)\frac{h^2}{Pa^2}$, $\bar{\sigma}_{yy} = \sigma_{yy}(a/2, a/2, h/4)\frac{h^2}{Pa^2}$ and $\bar{\tau}_{xz} = \tau_{xz}(0, /a2, 0)\frac{h}{Pa}$ of a simply supported cross-ply laminated square plate [0°/90°/90°/0°], with $E_1 = 25E_2$, $G_{12} = G_{13} = 0.5E_2$, $G_{23} = 0.2E_2$, $\nu_{12} = 0.25$.

a/h	Method	w	σ_{xx}	σ_{yy}	τ_{xz}
4	HSDT [40]	1.8937	0.6651	0.6322	0.2064
	FSDT [41]	1.7100	0.4059	0.5765	0.1398
	Elasticity [39]	1.9540	0.7200	0.666	0.2700
	RBF [15]	1.9783	0.6765	0.5872	0.2332
	Present (FEM Q4)	1.9086	0.7064	0.6270	0.2201
	CS-FEM Q4 (4 subcells)	1.9089	0.7067	0.6273	0.2201
10	HSDT [40]	0.7147	0.5456	0.3888	0.2640
	FSDT [41]	0.6628	0.4989	0.3615	0.1667
	Elasticity [39]	0.7430	0.5590	0.4030	0.3010
	RBF [15]	0.7325	0.5627	0.3908	0.3321
	Present (FEM Q4)	0.7193	0.5594	0.3904	0.2952
	CS-FEM Q4 (4 subcells)	0.7195	0.5597	0.3905	0.2952
100	HSDT [40]	0.4343	0.5387	0.2708	0.2897
	FSDT [41]	0.4337	0.5382	0.2705	0.1780
	Elasticity [39]	0.4347	0.5390	0.2710	0.3390
	RBF [15]	0.4307	0.5431	0.2730	0.3768
	Present (FEM Q4)	0.4302	0.5365	–	0.3285
	CS-FEM Q4 (4 subcells)	0.4304	0.5368	–	0.3285

Table 3
Transverse displacement $\bar{w} = w(a/2, a/2, h/2)$ at the center of a multilayered plate [0°/90°/0°] with $E_1 = 132.38$ GPa, $E_2 = E_3 = 10.756$ GPa, $G_{12} = 3.606$ GPa, $G_{13} = G_{23} = 5.6537$ GPa, $\nu_{12} = \nu_{13} = 0.24$, $\nu_{23} = 0.49$. A structured quadrilateral mesh with 20×20 elements.

$\bar{w}$	a/h				
	10	50	100	500	1000
Analytical (ESL-2) [5,6]	0.9249	0.7767	0.7720	0.7705	0.7704
MITC4 [8]	0.9195	0.7713	0.7666	0.7650	0.7650
Present (FEM Q4)	0.9232	0.7700	0.7651	0.7636	0.7635
CS-FEM Q4 (4 subcells)	0.9235	0.7703	0.7655	0.7639	0.7639

where n_x and n_y are the normals to the edge of the smoothing cell. Nguyen-Xuan et al. [34] did a systematic study on the influence of the number of subcells on the performance of Reissner–Mindlin plates. It was concluded that elements with one subcell exhibits two zero energy modes, while elements with two, three and four subcells maintain sufficient rank and no zero-energy modes. In this study, we use four subcells per element.

2.5. Shear locking

If the interpolation functions given for a QUAD-4 are used directly to interpolate the unknown displacement fields in deriving the shear strains (γ_{xz}, γ_{yz}) and the membrane strains ($\boldsymbol{\varepsilon}_{pG}$), the element will lock and show oscillations in the shear and the membrane stresses. The oscillations are due to the fact that the derivative functions of the out-of plate displacement do not match that of the rotations in the shear strain definition. To alleviate the locking phenomenon, the terms corresponding to the derivative of the out-of plate displacement must be consistent with the rotation terms. In this study, field redistributed shape functions are used to alleviate shear locking [32]. The field consistency requires that the transverse shear strains and the membrane strains must be interpolated in a consistent manner. If the element has edges which are aligned with the coordinate system (x,y), the terms in shear strains (γ_{xz}, γ_{yz}) are approximated by the following substitute shape functions [45]:

$$\widetilde{N}_1(\eta) = \frac{1}{4}[1-\eta \quad 1-\eta \quad 1+\eta \quad 1+\eta]$$
$$\widetilde{N}_2(\xi) = \frac{1}{4}[1-\xi \quad 1+\xi \quad 1+\xi \quad 1-\xi]. \tag{18}$$

Note that, no special integration rule is required for evaluating the shear terms. A numerical integration based on the 2×2 Gaussian rule is used to evaluate all the terms.

Remark 2.1. In this work, the curvature based smoothing technique proposed by Chen et al. [14] for meshfree methods and applied for plates by Nguyen et al. [37] is employed to approximate the extension and the bending strains.

Remark 2.2. Field consistent shape functions are employed to approximate the shear strains.

3. Numerical examples

In this section, we present the static response and the natural frequencies of laminated composite plates using four noded quadrilateral elements. In this study we use a hybrid displacement assumption, where in-plane displacements u and v are expressed as sinusoidal expansion in the thickness direction, and the transverse displacement, w is quadratic in the thickness direction. We refer to this theory as SINUS-W2. The displacements are expressed as:

$$\begin{aligned} u(x,y,z,t) &= u_o(x,y,t) + zu_1(x,y,t) + \sin\left(\frac{\pi z}{h}\right)u_2(x,y,t) \\ v(x,y,z,t) &= v_o(x,y,t) + zv_1(x,y,t) + \sin\left(\frac{\pi z}{h}\right)v_2(x,y,t) \\ w(x,y,z,t) &= w_o(x,y,t) + zw_1(x,y,t) + z^2w_2(x,y,t) \end{aligned} \tag{19}$$

where u_o, v_o and w_o are translations of a point at the middle-surface of the plate, w_2 is higher order translation, and u_1, v_1, u_3 and v_3

Table 4
Convergence of the normalized fundamental frequency $\Omega = \omega a^2/h\sqrt{\rho/E_2}$ of a simply supported cross-ply laminated square plate $(0°/90°)_s$ with $h/a = 0.2, \frac{E_1}{E_2} = 40, G_{12} = G_{13} = 0.6E_2, G_{23} = 0.5E_2, \nu_{12} = 0.25$.

Mesh	FEM-Q4	CSFEM-Q4			
		1 Subcell	2 Subcells	4 Subcells	8 Subcells
8×8	10.8901	10.8642	10.8726	10.8837	10.8858
10×10	10.8468	10.8303	10.8357	10.8427	10.8440
14×14	10.8093	10.8009	10.8036	10.8072	10.8079
20×20	10.7894	10.7853	10.7866	10.7883	10.7887
30×30	10.7788	10.7770	10.7775	10.7783	10.7785

Table 5
The normalized fundamental frequency $\Omega = \omega a^2/h\sqrt{\rho/E_2}$ of a simply supported cross-ply laminated square plate $(0°/90°)_s$ with $h/a = 0.2, \frac{E_1}{E_2} = 10, 20, 30$ or $40, G_{12} = G_{13} = 0.6E_2, G_{23} = 0.5E_2, \nu_{12} = 0.25$.

Method	Mesh	Subcell(s)	E_1/E_2			
			10	20	30	40
Liew [23]			8.2924	9.5613	10.3200	10.8490
Reddy, Khdeir [22]			8.2982	9.5671	10.3260	10.8540
FSDT [16]	21×21		8.2982	9.5671	10.3258	10.8540
HSDT [16] ($\nu_{23} = 0.18$)	21×21		8.2999	9.5411	10.2687	10.7652
Present FEM Q4	20×20		8.3651	9.5801	10.2980	10.7894
CS-FEM Q4	20×20	1	8.3604	9.5755	10.2937	10.7853
		2	8.3615	9.5767	10.2950	10.7866
		4	8.3639	9.5790	10.2970	10.7883
		8	8.3642	9.5793	10.2973	10.7887

Table 6
Variation of fundamental frequencies, $\Omega = \omega a^2/h\sqrt{\rho/E_2}$ with a/h for a simply supported square laminated plate $[0°/90°/90°/0°], \Omega = \omega a^2/h\sqrt{\rho/E_2}$, with $E_1/E_2 = 40$, $G_{12} = G_{13} = 0.6E_2$, $G_{23} = 0.5E_2$, $\nu_{12} = \nu_{13} = \nu_{23} = 0.25$.

Method	a/h					
	2	4	10	20	50	100
FSDT [47]	5.4998	9.3949	15.1426	17.6596	18.6742	18.8362
Model-1 (12dofs) [20]	5.4033	9.2870	15.1048	17.6470	18.6720	18.8357
Model-2 (9dofs) [20]	5.3929	9.2710	15.0949	17.6434	18.6713	18.8355
HSDT [40]	5.5065	9.3235	15.1073	17.6457	18.6718	18.8356
HSDT [43]	6.0017	10.2032	15.9405	17.9938	18.7381	18.8526
Present (FEM Q4)	5.4029	9.3005	15.1790	17.7578	18.7993	18.9657
CS-FEM Q4 (4 subcells)	5.4026	9.2998	15.1766	17.7540	18.7947	18.9611

denote rotations [46] and considers a quadratic variation of the transverse displacement w allowing for through-the-thickness deformations. The effect of the plate aspect ratio, the ply angle and the ratio of Young's modulus E_1/E_2 is numerically studied. Before proceeding with a detailed study on the effect of different parameters on the response of cross-ply laminated plates, the formulation developed here is compared against available results pertaining to static bending and free vibration of cross-ply laminated plates. In this study, smoothed element is denoted by CS-FEMQ4. The results with standard Q4 element with a field consistent approach is also presented, denoted by FEM-Q4. Table 1 shows the convergence of the central deflection of a simply supported cross-ply laminated square plate. The difference between a 30×30 structured mesh and a 20×20 structured mesh is <0.2%. Hence, in this study, a 20×20 structured quadrilateral mesh is used to model the full laminated plate. A comparison with other approaches and an elasticity solution is given in Table 2.

3.1. Static bending

The static analysis is conducted for cross-ply laminated plates with three and four layers under the following sinusoidal load:

$$p_z(x,y) = P_o \sin\left(\frac{\pi x}{a}\right) \sin\left(\frac{\pi y}{a}\right) \tag{20}$$

where P_o is the amplitude of the mechanical load. The origin of the coordinate system is located at the lower-left corner on the mid-plane. The physical quantities are non-dimensionalized by the following relations, unless otherwise mentioned:

$$\begin{aligned} &\bar{w} = w(a/2, a/2, 0)\frac{100h^3E_2}{Pa^4}; \quad \bar{\sigma}_{xx} = \sigma_{xx}(a/2, a/2, h/2)\frac{h^2}{Pa^2}; \\ &\bar{\sigma}_{yy} = \sigma_{yy}(a/2, a/2, h/4)\frac{h^2}{Pa^2}; \quad \bar{\tau}_{xx} = \tau_{xx}(0, a/2, h)\frac{h}{Pa}; \\ &\bar{\tau}_{xy} = \tau_{xy}(a, a, h/2)\frac{h^2}{Pa^2}. \end{aligned} \tag{21}$$

3.1.1. Four layer $(0°/90°)_s$ square cross-ply laminated plate under sinusoidal load

A square simply supported laminate of side a and thickness h, composed of four equally thick layers oriented at $(0°/90°)_s$ is considered. The plate is subjected to a sinusoidal vertical pressure given by Eq. (20). The material properties are as follows: $E_1 = 25E_2$; $G_{12} = G_{13} = 0.5E_2$; $G_{23} = 0.2E_2$; $\nu_{12} = 0.25$. For this example, a three-dimensional exact solution by Pagano [39] is available. In Table 2, we present results for the SINUS-W2 theory with strain smoothing and a field consistent approach. Also presented are the solutions from the standard 4-noded element with a field consistent approach, denoted by FEM-Q4. We compare the results with higher order plate theories [40,15], first order theory [41] and an exact solution [39]. The effect of plate the thickness is also shown in Table 2. It is clear that the first order shear deformation theories (FSDT) cannot be used for thick laminates. It can be seen that the results from the present formulation are in very good agreement with those in the literature and very precise transverse displacements and stresses are obtained. The main features of the present formulation are: (1) theories from ESL to higher order layer descriptions can be implemented within a single code (since it is based on CUF); (2) the strain smoothing technique reduces the computational effort and also improves the accuracy of the field variables and (3) the present formulation is insensitive to shear locking.

3.1.2. Three layer $(0°/90°/0°)$ square cross ply laminated plate under sinusoidal load

In this case, a square laminate of side a and thickness h, composed of three equally thick layers oriented at $(0°/90°/0°)$ is considered. It is simply supported on all edges and subjected to a sinusoidal vertical pressure of the form given by Eq. (20). The material properties for this example are: $E_1 = 132.38$ GPa, $E_2 = E_3 = 10.756$ GPa, $G_{12} = 3.606$ GPa, $G_{13} = G_{23} = 5.6537$ GPa, $\nu_{12} = \nu_{13} = 0.24$, $\nu_{23} = 0.49$. In Table 3, we present results for the SINUS-W2 theory with strain smoothing and a field consistent approach. The results from the present formulation are compared with the

analytical solution [5,6] and the MITC4 formulation [8]. It can be seen that the numerical results from the present formulation are found to be in good agreement with the existing solutions. Moreover, the present formulation shows an improvement in the accuracy of the field variables when compared to other formulations and is insensitive to shear locking.

3.2. Free vibration – cross-ply laminated plates

In this example, all layers of the laminate are assumed to be of the same thickness, density and made up of the same linear elastic material. The following material parameters are considered for each layer

$$\frac{E_1}{E_2} = 10, 20, 30, \text{ or } 40; \quad G_{12} = G_{13} = 0.6E_2; \quad G_3 = 0.5E_2; \nu_{12} = 0.25.$$

The subscripts 1 and 2 denote the directions normal and the transverse to the fiber direction in a lamina, which may be oriented at an angle to the plate axes. The ply angle of each layer is a measure from the global x-axis to the fiber direction. The example considered is a simply supported square plate with cross-ply lamination $(0°/90°)_s$. The thickness and the length of the plate are denoted by h and a, respectively. The thickness-to-span ratio $h/a = 0.2$ is employed in the computations. In this study, we present the non dimensionalized free flexural frequencies as, unless specified otherwise:

$$\Omega = \omega \frac{a^2}{h}\sqrt{\frac{\rho}{E_2}}$$

Table 4 shows the convergence of the normalized fundamental frequency of a simply supported cross-ply laminated square plate. In this study, a 20×20 structured quadrilateral mesh is used to model the full laminated plate. Table 5 lists the fundamental frequency for a simply supported cross-ply laminated square plate with $h/a = 0.2$ and for different Young's modulus ratios, E_1/E_2. It can be seen that the results from the present formulation are in very close agreement with the values of [22] based on higher order theory, the meshfree results of Liew et al. [23] and Ferreira et al. based on FSDT and higher order theories with radial basis functions [16]. The effect of plate thickness on the fundamental frequency is shown in Table 6. It can be seen that the results agree with the results available in the literature. The present formulation is insensitive to shear locking.

4. Conclusion

In this article, the cell based smoothing technique for implementation of the Carrera Unified Formulation was detailed and discussed. The efficiency and accuracy of the present approach is demonstrated with few numerical examples. The shear locking is suppressed by employing a field consistent approach. This improved finite element technique shows insensitivity to shear locking and produce excellent results in static bending and free vibration of cross-ply laminated plates.

References

[1] Bathe KJ, Dvorkin EN. A four-node plate bending element based on Mindlin/Reissner plate theory and a mixed interpolation. Int J Numer Meth Eng 1985;21:367–83.

[2] Babuška I. The finite element method with Lagrangian multipliers. Num Math 1973;20:179–92.

[3] Bordas S, Natarajan S, Kerfriden P, Augarde CE, Roy Mahapatra D, Rabczuk T, et al. On the performance of strain smoothing for quadratic and enriched finite element approximation (XFEM/GFEM/PUFEM). Int J Numer Meth Eng 2011;86:637–66.

[4] Bordas SPA, Natarajan S. On the approximation in the smoothed finite element method (SFEM). Int J Numer Meth Eng 2010;81:660–70.

[5] Carrera E. Evaluation of layer-wise mixed theories for laminated plates analysis. AIAA J 1998;26:830–9.

[6] Carrera E. Developments, ideas and evaluations based upon the Reissner's mixed variational theorem in the modelling of multilayered plates and shells. Appl Mech Rev 2001;54:301–29.

[7] Carrera E. Theories and finite elements for multilayered plates and shells: a unified compact formulation with numerical assessment and benchmarking. Arch Comput Meth Eng 2003;10:215–96.

[8] Carrera E, Cinefra M, Nali P. MITC technique extended to variable kinematic multilayered plate elements. Compos Struct 2010;92:1888–95.

[9] Cazes F, Meschke G. An edge based imbricate finite element method (EI-FEM) with full and reduced integration. Comput Struct 2012;106–107:154–75.

[10] Cinefra M, Chinosi C, Della Croce L. MITC9 shell elements based on refined theories for the analysis of isotropic cylindrical structures. Mech Advan Mater Struct 2013;20:91–100.

[11] Cinefra M, Carrera E. Shell finite elements with different through-the-thickness kinematics for the linear analysis of cylindrical multilayered structures. Int J Numer Meth Eng 2013;93:160–82.

[12] Chinosi C, Cinefra M, Della Croce L, Carrera E. Reissner's mixed variational theorem toward MITC finite elements for multilayered plates. Compos Struct 2013;99:443–52.

[13] Carrera E, Demasi L. Classical and advanced multilayered plate elements based upon PVD and RMVT. Part 1: derivation of finite element matrices. Int J Numer Meth Eng 2002;55:191–231.

[14] Chen JS, Wang HP. Some recent improvements in meshfree methods for incompressible finite elasticity boundary value problems with contact. Comput Mech 2000;25:137–56.

[15] Ferreira AJM, Carrera E, Cinefra M, Roque CMC. Radial basis functions collocation for the bending and free vibration analysis of laminated plates using the Reissner–Mixed variational theorem. Euro J Mech – A/Solids 2012;39:104–12.

[16] Ferreira AJM, Roque CMC, Carrera E, Cinefra M. Analysis of thick isotropic and cross-ply laminated plates by radial basis functions and a unified formulation. J Sound Vib 2011;330:771–87.

[17] He ZC, Cheng AG, Zhang GY, Zhong ZH, Liu GR. Dispersion error reduction for acoustic problems using the edge-based smoothed finite element method (ES-FEM). Int J Numer Meth Eng 2011;86:1322–38.

[18] Hughes TJR, Cohen M, Haroun M. Reduced and selective integration techniques in finite element method of plates. Nucl Eng Des 1978;46:203–22.

[19] Kant T, Swaminathan K. Estimation of transverse/interlaminar stresses in laminated composites – a selective review and survey of current developments. Compos Struct 2000;49:65–75.

[20] Kant T, Swaminathan K. Analytical solutions for free vibration of laminated composite and sandwich plates based on a higher-order refined theory. Compos Struct 2001;53(1):73–85.

[21] Khandan R, Noroozi S, Sewell P, Vinney J. The development of laminated composite plate theories: a review. J Mater Sci 2012;47:5901–10.

[22] Khdeir AA, Librescu L. Analysis of symmetric cross-ply elastic plates using a higher-order theory: part II: buckling and free vibration. Compos Struct 1988;9:259–77.

[23] Liew KM, Huang YQ, Reddy JN. Vibration analysis of symmetrically laminated plates based on FSDT using the moving least squares differential quadrature. Comput Meth Appl Mech Eng 2003;192:2203–22.

[24] Liu G, Nguyen-Thoi T, Lam K. A novel alpha finite element method (αfem) for exact solution to mechanics problems using triangular and tetrahedral elements. Comput Meth Appl Mech Eng 2008;197:3883–97.

[25] Liu G, Nguyen-Thoi T, Lam K. An edge-based smoothed finite element method (ES-FEM) for static, free and forced vibration analyses of solids. J Sound Vib 2009;320:1100–30.

[26] Liu G, Nguyen-Thoi T, Nguyen-Xuan H, Lam K. A node based smoothed finite element (NS-FEM) for upper bound solution to solid mechanics problems. Comput Struct 2009;87:14–26.

[27] Liu GR, Nguyen-Thoi T, Dai KY, Lam KY. Theoretical aspects of the smoothed finite element method (SFEM). Int J Numer Meth Eng 2007;71:902–30.

[28] Liu GR, Dai KY, Nguyen TT. A smoothed finite element for mechanics problems. Comput Mech 2007;39:859–77.

[29] Mallikarjuna, Kant T. A critical review and some results of recently developed refined theories of fibre reinforced laminated composites and sandwiches. Compos Struct 1993;23:293–312.

[30] Murukami H. Laminated composite plate theory with improved in-plane responses. J Appl Mech 1986;53:661–6.

[31] Carrera nad E, Demasi L. Classical and advanced multilayered plate elements based upon PVD and RMVT. Part 2: numerical implementations. Int J Numer Meth Eng 2002;55:253–91.

[32] Natarajan S, Baiz Pedro M, Bordas S, Rabczuk T, Kerfriden P. Natural frequencies of cracked functionally graded material plates by the extended finite element method. Compos Struct 2011;93:3082–92.

[33] Nguyen-Thoi T, Liu G, Lam K, Zhang G. A face-based smoothed finite element method (FS-FEM) for 3D linear and nonlinear solid mechanics using 4-node tetrahedral elements. Int J Numer Meth Eng 2009;78:324–53.

[34] Nguyen-Xuan H, Bordas S, Nguyen-Dang H. Smooth finite element methods: convergence, accuracy and properties. Int J Numer Meth Eng 2008;74:175–208.

[35] Nguyen NT, Rabczukm T, Nguyen-Xuan H, Bordas S. A smoothed finite element method for shell analysis. Comput Meth Appl Mech Eng 2008;198:165–77.

[36] Nguyen-Xuan H, Liu GR, Bordas S, Natarajan S, Rabczuk T. An adaptive singular ES-FEM for mechanics problems with singular field of arbitrary order. Comput Meth Appl Mech Eng 2013;253:252–73.
[37] Nguyen-Xuan H, Rabczuk T, Bordas S, Debongnie JF. A smoothed finite element method for plate analysis. Comput Meth Appl Mech Eng 2008;197:1184–203.
[38] Noor AK, Burton WS. Assessment of shear deformation theories for multilayered composite plates. ASME Appl Mech Rev 1989;42:1–13.
[39] Pagano NJ. Exact solutions for rectangular bidirectional composites and sandwich plates. J Compos Mater 1970;4:20–34.
[40] Reddy JN. A simple higher order theory for laminated composite plates. ASME J Appl Mech 1984;51:745–52.
[41] Reddy JN, Chao WC. A comparison of closed-form and finite-element solutions of thick laminated anisotropic rectangular plates. Nucl Eng Des 1981;64:153–67.
[42] Reddy JN, Robbins Jr DH. Theories and computational models for composite laminates. Appl Mech Rev 1994;47:147–69.
[43] Senthilnathan NR, Lim KH, Lee KH, Chow ST. Buckling of shear deformable plates. AIAA J 1987;25(9):1268–71.
[44] Simo JC, Hughes TJR. On the variational foundation of assumed strain methods. J Appl Mech (ASME) 1986;53:51–4.
[45] Somashekar BR, Prathap G, Ramesh Babu C. A field-consistent four-noded laminated anisotropic plate/shell element. Comput Struct 1987;25:345–53.
[46] Touratier M. An efficient standard plate theory. Int J Eng Sci 1991;29:901–16.
[47] Whitney JM, Pagano NJ. Shear deformation in heterogeneous anisotropic plates. ASME J Appl Mech 1970;37(4):1031–6.
[48] Wu Z, Chen R, Chen W. Refined laminated composite plate elemen based on global–local higher-order shear deformatio theory. Compos Struct 2005;70:135–52.
[49] Wu SC, Liu GR, Cui XY, Nguyen TT, Zhang GY. An edge-based smoothed point interpolation method ES-PIM for heat transfer analysis of rapid manufacturing system. Int J Heat Mass Trans 2010;53:1938–50.